The Abdus Salam
International Centre for Theoretical Physics

United Nations
Educational, Scientific and
Cultural Organization

IAEA
International Atomic Energy Agency

SMR/1849-23

Conference and School on Predictability of Natural Disasters for our Planet in Danger. A System View; Theory, Models, Data Analysis

25 June - 6 July, 2007

The Preferred Structure of the Interannual Indian Monsoon Variability

Davis Straus
George Mason University Calverton, USA

Pure appl. geophys. 164 (2007) 1–16
DOI 10.1007/s00024-007-0248-x

Pure and Applied Geophysics

The Preferred Structure of the Interannual Indian Monsoon Variability

DAVID M. STRAUS[1] and V. KRISHNAMURTHY[2]

Abstract—The leading empirical orthogonal function (EOF) of the June-Sept. mean, rotational horizontal wind at 850 hPa and 200 hPa (over the region 12.5°S–42.5°N, 50°E–100°E) from 56 years (1948–2003) of reanalysis (from the National Centers for Environmental Prediction) shows strong anti-cyclonic circulation at upper levels, strong Indian Ocean cross-equatorial flow and on-shore flow over western India at lower levels . The associated principal component (PC) is correlated at the 0.75 level with the seasonal mean observed Indian Monsoon rainfall (IMR). Composite differences of vertically integrated divergence (surface to 800 hPa) and vorticity (surface to 500 hPa) between "strong" years (PC-1 exceeds one standard deviation σ) and "weak" years (PC-1 less than $-\sigma$) suggest increased rising motion and storminess over the Bay of Bengal and central India. Composite difference maps of station rainfall from the India Meteorological Department (IMD) between strong years and normal years (weak years and normal years) are statistically significant over central India, with strong (weak) years associated with increased (decreased) precipitation. In both cases the maps of rainfall anomalies are of one sign throughout India. The correlation of PC-1 with global seasonal mean SST is strong and negative over the eastern equatorial Pacific, but positive in a surrounding horse-shoe like region. Significant negative correlation occurs in the northwestern Indian Ocean. The lag/lead correlation between the NINO3 SST index and PC-1 is similar to but stronger than the NINO3/IMR correlation. Modest (but significant) negative correlation is seen when NINO3 leads PC-1 (or IMR) by one-two months. Strong negative correlation is seen when PC-1 (or IMR) leads NINO3. The projections of running five-day means of horizontal rotational winds at 850 and 200 hPa onto EOF-1 (after removing the seasonal mean for each year) were pooled for strong, normal and weak years. The strong and normal year pdfs are nearly indistinguishable, but the weak year pdf has more weight for moderate negative values and in both extreme tails and shows some hint of bi-modality.

Key words: ■■

1. Introduction

The relationship between the seasonal mean Indian monsoon and the intra-seasonal fluctuations has been discussed extensively both from the point of view of the precipitation and the large-scale circulation (KRISHNAMURTHY and SHUKLA,

[1] Department of Climate Dynamics, George Mason University, Fairfax, Virginia, U.S.A.
E-mail: straus@cola.iges.org.
[2] Center for Ocean-Land-Atmosphere Studies, Institute of Global Environment and Society, Inc., Calverton, Maryland, U.S.A.

S B 0 1 0 2 4 8 B
Journal number | Manuscript number
Dispatch: 19.5.2007 Journal: Pure and applied Geophysics No. of pages: 16
Author's disk received ☑ Used ☑ Corrupted ☐ Mismatch ☐ Keyed ☐

2000; SPERBER *et al.*, 2000; GOSWAMI and AJAYA-MOHAN, 2001). The basic questions that underlie much of this research are whether the seasonal mean is the residual of chaotic weather systems and their low-frequency intra-seasonal modulation, the "residual hypothesis", or whether the seasonal mean has a separate physical origin related to the slowly varying boundary conditions such as the sea-surface temperature (SST), soil moisture and snow cover, the "boundary forced hypothesis" (CHARNEY and SHUKLA, 1981; KRISHNAMURTHY and SHUKLA, 2000, hereafter KS). The well-known links of seasonal mean rainfall to Pacific SST related to the El-Niño Southern Oscillation (ENSO) as well as to winter/spring Eurasian snow cover are reviewed by WEBSTER *et al.* (1998).

The implications of this debate for potential predictability are profound, for the 'residual' hypothesis implies very little predictability for seasonal means. According to the boundary-forced hypothesis, the slowly varying land and ocean states play an important role, so there is some potential predictability in the monsoon system for the seasonal mean.

One approach taken to resolve this debate has been to seek a few large-scale seasonal mean circulation patterns that are associated with the interannual variability of the seasonal mean all-India monsoon rainfall. The existence of one or two such patterns that are highly correlated with the Indian monsoon rainfall on interannual time scales would support the boundary forced hypothesis. On the other hand, the residual hypothesis would imply that a number of patterns should be involved, for the structure of the intra-seasonal variability is rather complex, involving a number of space and time scales (as in KS and SPERBER *et al.*, 2000). GOSWAMI and AJAYA-MOHAN (2001) find the leading empirical orthogonal function (EOF) of monsoon seasonal mean 850 hPa horizontal winds from a 40-year record obtained from the reanalyses of the National Centers for Environmental Prediction/National Center for Atmospheric Research (KALNAY *et al.*, 1996; hereafter NCEP). The corresponding time series (principle component, or PC) has a correlation of 0.62 with the seasonal mean all-India Monsoon Rainfall (IMR) given by PARTHASARATHY *et al.* (1995). A similar calculation is presented by SPERBER *et al.* (2000), who show that the leading PC has a significant trend associated with it.

An alternate approach is to identify the key aspects of the seasonal mean circulation which should be related to the seasonal mean IMR on a physical basis. WEBSTER and YANG (1992) and WANG and FAN (1999) identify indices based on the dominance of the first baroclinic mode in monsoon dynamics. These indices involve the vertical shear of the zonal wind over the monsoon region. GOSWAMI *et al.* (1999) focus on the local Hadley cell associated with the monsoon to define an index based on the meridional wind shear. (Details of these indices and their correlation with the IMR will be discussed later in the paper.).

One purpose of this paper is to show that by combining the two previous approaches (EOF analysis of a single level and consideration of vertical shear), we can obtain a single, multi-level seasonal mean circulation pattern (or mode) that is

closely associated with the seasonal mean IMR over a period of 56 years. Another purpose is to examine the boundary forced hypothesis by discussing the geographic distribution of observed seasonal mean Indian rainfall associated with this mode, as well as the correlation with global SST. The relationship of the intra-seasonal fluctuations to this single preferred seasonal mean mode is studied by estimating the probability distribution function (pdf) of the projections of these fluctuations on this mode for each year. In particular we study the change of the pdf from "strong" to "weak" monsoon years, these being defined from the PC of the leading mode.

Section 2 describes the data sets and EOF analysis methods, while Section 3 shows the circulation (winds, vorticity, divergence) associated with the two leading EOFs. Maps of observed Indian rainfall associated with the leading EOF are shown in Section 4, while Section 5 shows the relationship of the leading EOF to global SST. The pdfs of intra-seasonal fluctuations projected onto the leading EOF are discussed in Section 6, and Discussion and Conclusions are given in Section 7.

2. Data and Method of Analysis

a. Rainfall

The seasonal mean (June – September) rainfall integrated over India for the period 1948–2003 was obtained from the Indian Institute of Tropical Meteorology (PARTHASRATHY *et al.*, 1995). We refer to this as IMR, although other studies have called this the all-India rainfall. This time series was detrended in the manner described below.

Maps of rainfall were obtained from the data set created by the India Meteorological Department (IMD) using daily observations ranging up to 6329 rain gauge stations. The station data were converted into gridded data on a 1° lon. × 1° lat. grid covering land points over India for the period 1951–2003 using a suitable interpolation scheme (RAJEEVAN *et al.*, 2005). For this study, the seasonal mean and anomaly for June to September (JJAS) season were computed from the daily data.

b. Circulation Fields

The seasonal mean (JJAS) fields of horizontal wind (u,v) were obtained from the NCEP reanalysis data set for the 56–year period 1948–2003. The input to the EOF calculations (see subsection e below) consisted of the seasonal mean rotational components of (u,v) at the 850 hPa and 200 hPa levels over the region 12.5°S–42.5°N, 50°E–100°E for the 56-year period. These components were detrended prior to the EOF calculation (see subsection c). The detrending and removal of the divergent components of the wind fields were motivated by: (i) the well-known

temporal inhomogeneity in the NCEP reanalysis data set, particularly in the divergent component of the circulation (KINTER *et al.*, 2004); and (ii) the artificial correlation that can be introduced by the presence of trends.

The wind components were interpolated from the original grid to a nearly equivalent Gaussian T42 grid (2.8125° lon. × ~2.8° lat.) in order to compute the rotational components.

For the composites shown in Section 3, the seasonal mean horizontal winds, vorticity and divergence were used on the 2.5° lat. × 2.5° lon. grid at the 13 levels: 1000, 925, 850, 700, 600, 500, 400, 200, 250, 200, 150, 100 and 70 hPa for the same 56-year period 1948–2003. These data were also detrended, as in subsection c.

c. Detrending

The 56-year seasonal mean time series of IMR, rotational winds at two levels, and full winds at 13 levels, were all detrended by removing the climatological mean, the linear trend and the parabolic (in time) component. These three components correspond to the first three Legendre functions in time, and so can be computed and removed in a simple manner (see STRAUS, 1983 for more details). The linear trend (not shown) of the 200 hPa winds is dominated by decreasing easterlies (increasing westerlies) near and south of the equator (near 30°N) at a rate of roughly 0.3% per year at most. At 850 hPa, the trend shows increasing easterlies and northerlies off the southwest coast of India (at the rate of roughly 0.5% per year), thus a weakening of the on-shore monsoon flow. The parabolic component is extremely weak except near the northern boundary of our domain. (A caveat here is that the trend is removed at each point whether or not it is statistically significant, so that each grid point was treated consistently.)

d. SST Data

The SST data used in this study came from the HadIsst1 (1.1 version) data set created by the Hadley Centre for Climate Prediction and Research (RAYNER *et al.*, 2003). The monthly mean SST data are provided on a 1° lon. × 1° lat. global grid and we used the data covering the period 1948–2003. The JJAS means and anomalies of SST were computed from the monthly means. The NINO3 index is defined as the areal average of SST for 5°S–5°N, 150°W–90°W.

e. EOF Analysis

For each JJAS mean, the 200 and 850 hPa fields of rotational wind (u_r, v_r) were combined into a single data vector. Each grid point was weighted by the square-root of the cosine of latitude; no other weighting was used. From the time series ($N = 56$) of these vectors, the covariance matrix over the region indicated in subsection b was constructed, and the ortho-normal set of eigenvectors (or EOFs) determined.

Projection of the time series of data vectors onto each eigenvector yielded the (dimensional) principal components (PCs).

The fields associated with the leading EOFs were computed on the basis of composites. For the full horizontal wind fields, divergence and vorticity at 13 levels (see subsection b), positive (negative) composites were obtained as the mean over all years for which the appropriate PC was greater (less) than +1.0 (−1.0) standard deviation.

3. The Leading EOFs

The space-time variance explained by the leading EOFs is reported in Table 1 (in terms of percent), along with the uncertainty due to sampling error. (NORTH *et al.*, 1982). The first EOF (25% explained variance) is clearly distinct from the higher order EOFs, while the significance of EOF-2 (15% explained variance) is marginal.

Differences between positive and negative composites of the full horizontal wind field associated with EOF-1 are shown in Figures 1a and 1b for the 850 and 200 hPa levels. The positive (negative) composites are defined as the mean over the 7 (12) years: 1959, 1961, 1964, 1970, 1973, 1978 and 1985 (1951, 1957, 1963, 1965, 1969, 1972, 1974, 1979, 1982, 1987, 1997, and 2002). The 10% significance level (based on a two-sided t-test) is indicated by the shading.

The lower level wind field indicates anti-cyclonic flow just north of the equator, and generally cyclonic flow in the monsoon trough region. There is an enhancement of the cross-equatorial flow in the Arabian Sea and the on-shore flow over western India. The upper level flow is dominated by a strong anti-cyclonic center at about 35°N, 65°E, leading to strong north-easterly flow over India. The three-dimensional structure of the EOF-1 composite maps is consistent with the fields of correlation of Bay of Bengal convection with upper and lower level winds presented in WANG and FAN (1999).

Table 1

EOF Variance. The space-time variance explained by the leading EOFs, in percent terms. The range of explained variance includes the uncertainty as estimated from NORTH et al. (1981). The correlation of the corresponding PC with the IMR is given in the last column. Values significant at the 5% level are bold faced

	Explained Variance (%)	Range of Exp. Var (%)	Correlation with IMR
EOF-1	25.2	30–20	**0.75**
EOF-2	15.3	18–12	−0.07
EOF-3	10.8	13–9	0.15
EOF-4	6.6	8–5	0.14

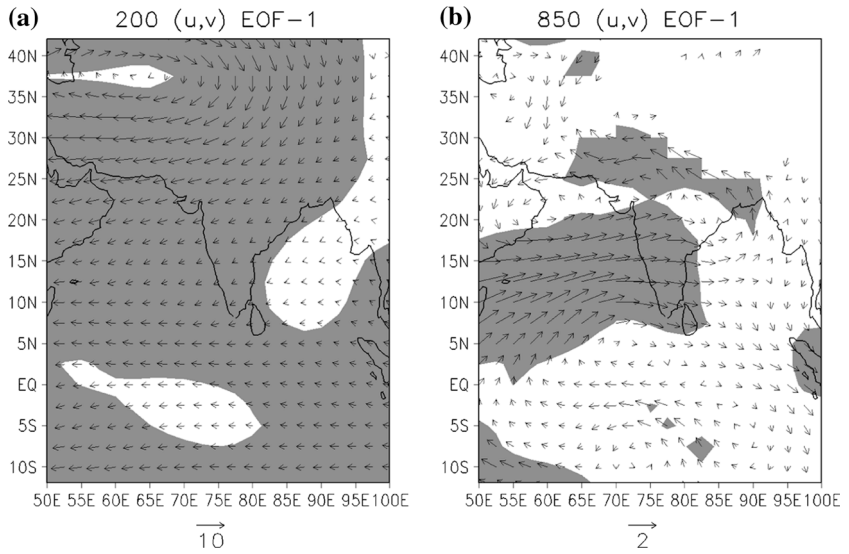

Figure 1
Composite differences of full horizontal winds for 200 hPa (a) and 850 hPa (b). Composite differences are defined as the difference between the mean of all (7) years for which PC-1 $>$ one standard deviation (σ) and the mean of all (12) years for which PC-1 $< -\sigma$. Shading denotes 10% significance using a two-sided t-test. Reference vectors show the magnitude (in m/sec) in each case.

The panels in Figure 2 show the composite differences of the mass-weighted vertical integral of: divergence from the surface to 800 hPa (Fig. 2a), of vorticity from the surface to 500 hPa (Fig. 2b) and of the divergence from 275 to 85 hPa[1] (Fig. 2c). To the extent that the time mean vorticity integrated over the lower half of the atmosphere is a measure of the presence of cyclonic monsoon disturbances, Figure 2b suggests a storm path from the Bay of Bengal westward across India and into the Arabia Sea, consistent with Figure. 1b, and consistent with the lower level divergence in Figure 2a. The upper level divergence suggests deep convection over the equator (which is confirmed by the vertical velocity composites, not shown), and the presence of upward motion over the higher elevations of Pakistan.

Composite differences of EOF-2 for the total wind field at 850 hPa and the vorticity, integrated from the surface to 500 hPa, are shown in Figures 3a and 3b. The circulation again shows enhanced cross-equatorial and on-shore Indian flow, although for a narrower region of the western Indian Ocean than was the case for EOF-1. (The area of high statistical significance is also smaller.) Over the northwestern Arabian Sea the winds are actually northerly. The lower troposphere integrated vorticity (Fig. 3b) suggests increased storminess over a region near Bangladesh and one in the northwestern Indian Ocean.

[1] The boundaries of the vertical integration were picked to be halfway between two analysis levels.

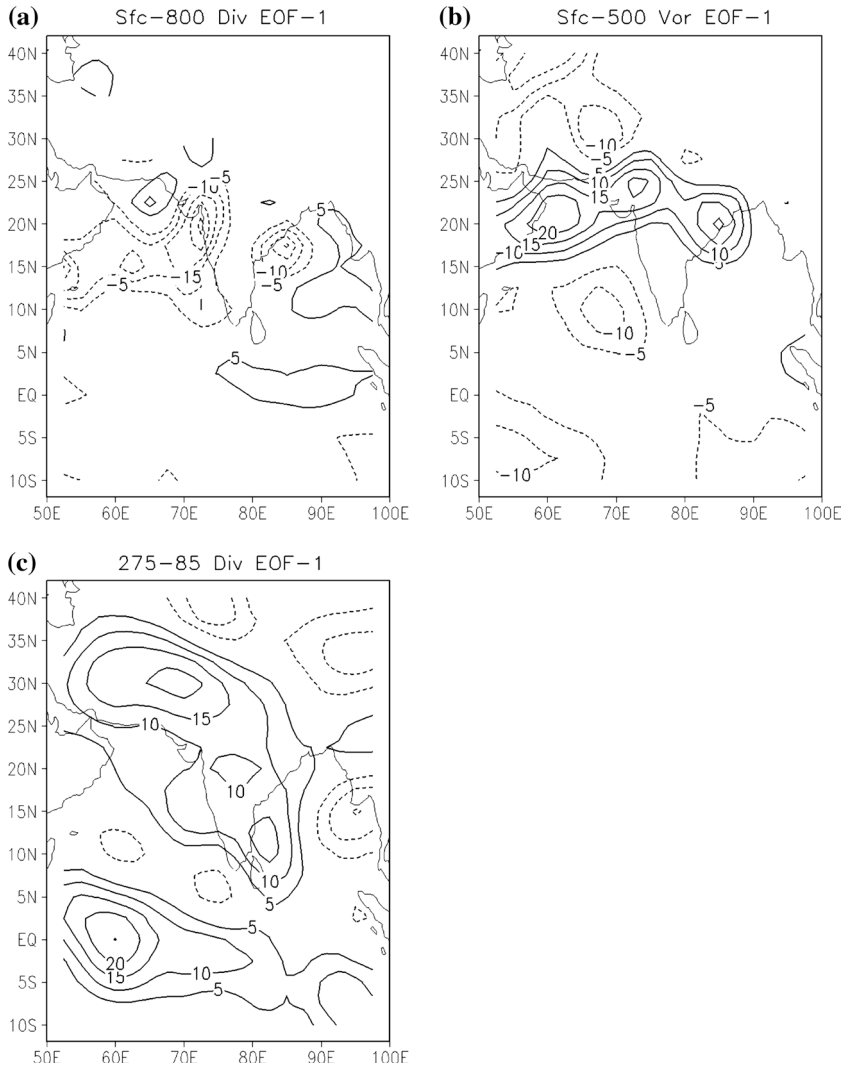

Figure 2

Composite differences of mass-weighted vertical integral of (a) Divergence (from the surface to 800 hPa), (b) vorticity (from the surface to 500 hPa), (c) divergence (from 275–85 hPa). Composite difference is the difference between the mean of all (7) years for which PC-1 $>$ one standard deviation (σ) and the mean of all (12) years for which PC-1 $< -\sigma$. Contour interval is 1.0×10^{-4} kg/(m^2 s) in (a) and (c), 1.0×10^{-3} kg/(m^2 s) in (b). Zero contour omitted.

The leading two PCs are presented in standardized form in Figures 4a and 4b as the blue curve in each case. The standardized (and detrended) IMR is shown as the red curve. From Figure 4a it is clear that PC-1 and IMR are highly correlated (value

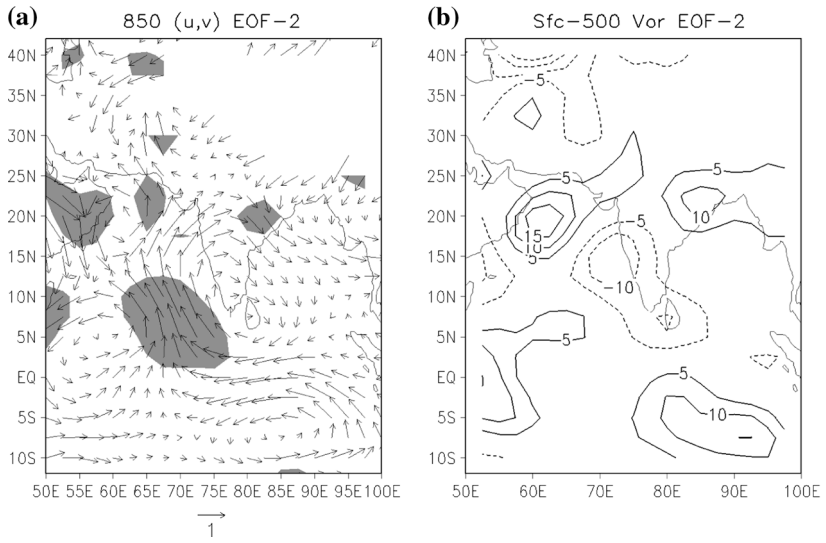

Figure 3
Composite difference of full 850 hPa horizontal wind (a) and vertical mass-weighted integral of vorticity from the surface to 500 hPa (b) for EOF-2. Composite difference is the difference between the mean of all (9) years for which PC-2 > one standard deviation (σ) and the mean of all (9) years for which PC-2 < $-\sigma$. Contour interval is 1.0×10^{-4} kg/(m^2 s) in (b). Reference vector in (a) is in m/sec. Shading denotes 10% significance using a two-sided t-test. Zero contour omitted in (b).

of 0.75); most of the extreme values of the IMR are well-matched by variations in PC-1. This is not the case for PC-2.

4. Rainfall Composites

Composite maps of seasonal mean rainfall anomaly over continental India were computed separately for the years in which PC-1 was greater than one standard deviation (Strong Composite), and for years in which PC-1 was less than minus one standard deviation (Weak Composite). These maps are shown in Figures 5a and 5b, along with the regions for which the composites meet the 10% significance level (based on a two-sided t-test) in Figures 5c and 5d. The strong composite shows enhanced rainfall along India (20°N–25°N), along the west coast, and to the north. The sign of the anomaly is generally the same over all of India. The weak composite shows generally reduced rainfall over the same regions, with the anomaly again being of predominantly one sign. Note that while the strong composite values are generally larger, the weak composite achieves statistical significance over a much larger region.

The structure of both composites is similar to the map of composite rainfall shown by KS, based entirely on the seasonal mean IMR for the extended period 1901–1970. The composite maps look quite different, however, from the difference

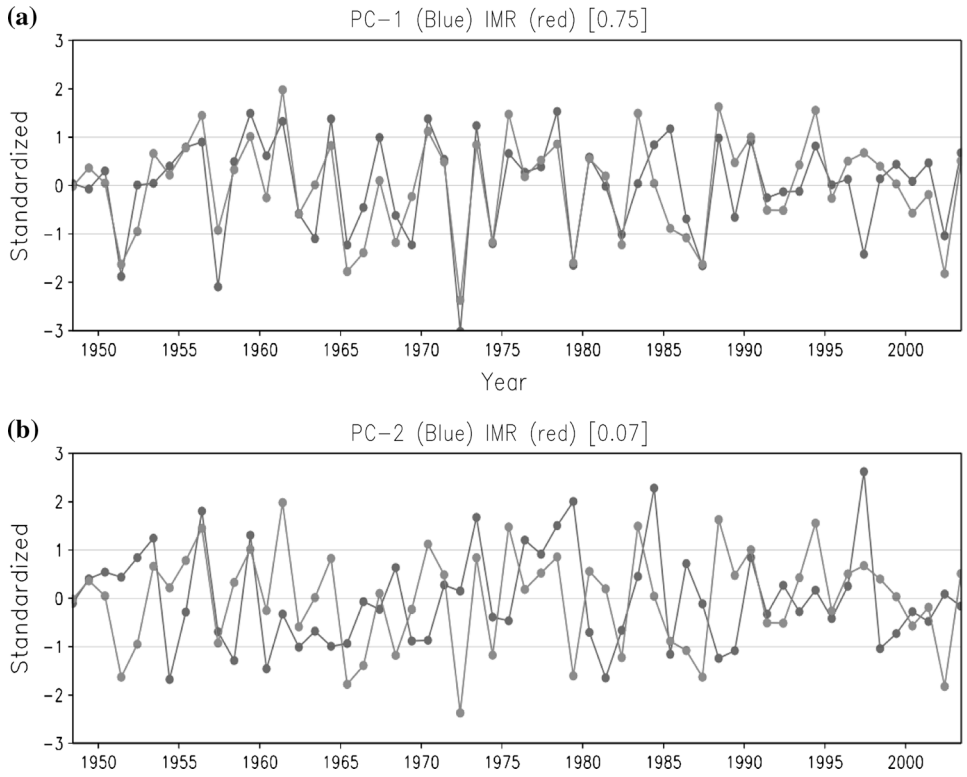

Figure 4
PC-1 (a) and PC-2 (b) shown in blue curves. IMR is shown in red curves. All series are defined for JJAS seasonal mean only, and are standardized. The correlation between the PC and IMR is shown in brackets for each panel. Thin lines show –1, 0, 1 standard deviation.

map of intra-seasonal active phase composite and break phase composite rainfall anomalies shown by KS. The latter shows much of southeastern and northern India with a rainfall anomaly of opposite sign to that of central India.

5. Global SST Relationships

The association of the leading EOF with the global distribution of seasonal mean SST can be assessed from Figure 6b, which shows the point-wise temporal correlation of SST with PC-1. (A correlation of absolute value greater than 0.30 is significant at the 2% level.) The familiar ENSO pattern is predominant in Figure 6b, along with a region of strong correlation in the Northwest Pacific. The significant negative correlation in the western Indian Ocean is indicative of two possible ways in which the atmosphere forces the ocean: (i) Strong monsoon winds lead to

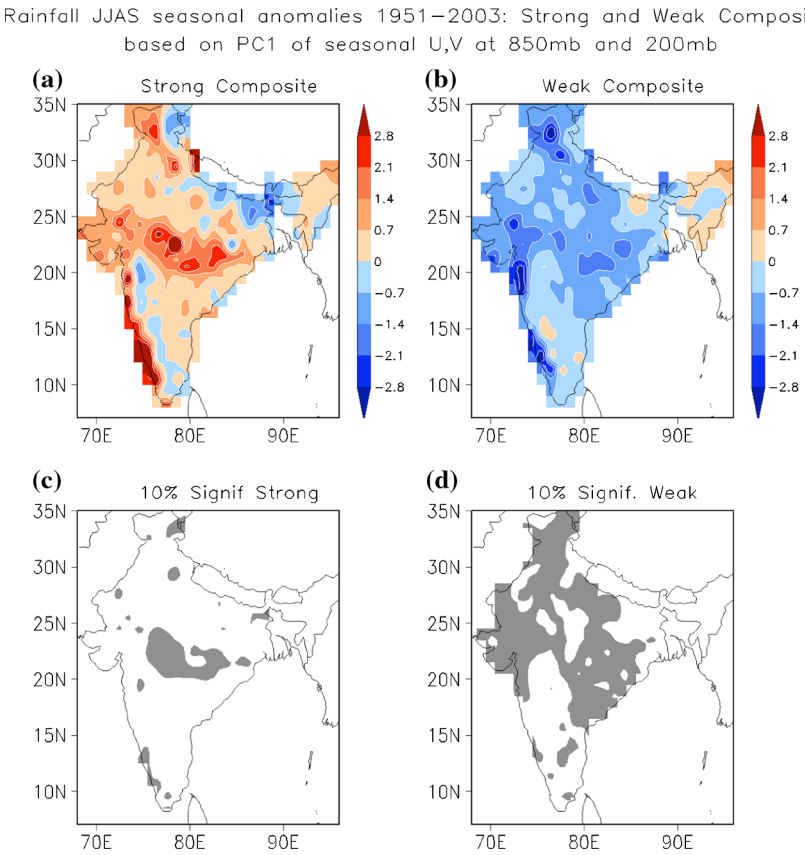

Figure 5

(a) Difference of IMD rainfall between the mean of all strong (7) years for which PC-1 > one standard deviation (σ) and the mean of all "neutral" (37) years for which $-\sigma <$ PC-1 $< \sigma$. (b) Difference of IMD rainfall between the mean of all weak (11) years for which PC-1 $< -\sigma$ and the mean of all (37) neutral years. The regions shaded in (c) and (d) show anomalies that are statistically significant at the 10% level. Units are mm/day.

evaporative cooling, and (ii) the winds force enhanced coastal upwelling. These features associated with the leading EOF are well known to be associated with the strength of the seasonal mean Indian monsoon as measured by the IMR, as discussed in WEBSTER *et al.* (1998). While the correlation pattern over the Indian Ocean may seem to involve a dipole-like structure (see e.g., SAJI *et al.*, 1999), KRISHNAMURTHY and KIRTMAN (2003) argue that SST variability in this region is linked dynamically to that in the Pacific.

The temporal lead-lag relationship between the IMR and ENSO is summarized by the green line in Figure. 6a, which shows the lag correlation of monthly anomalies of the NINO3 index with the JJAS seasonal mean anomaly of IMR.

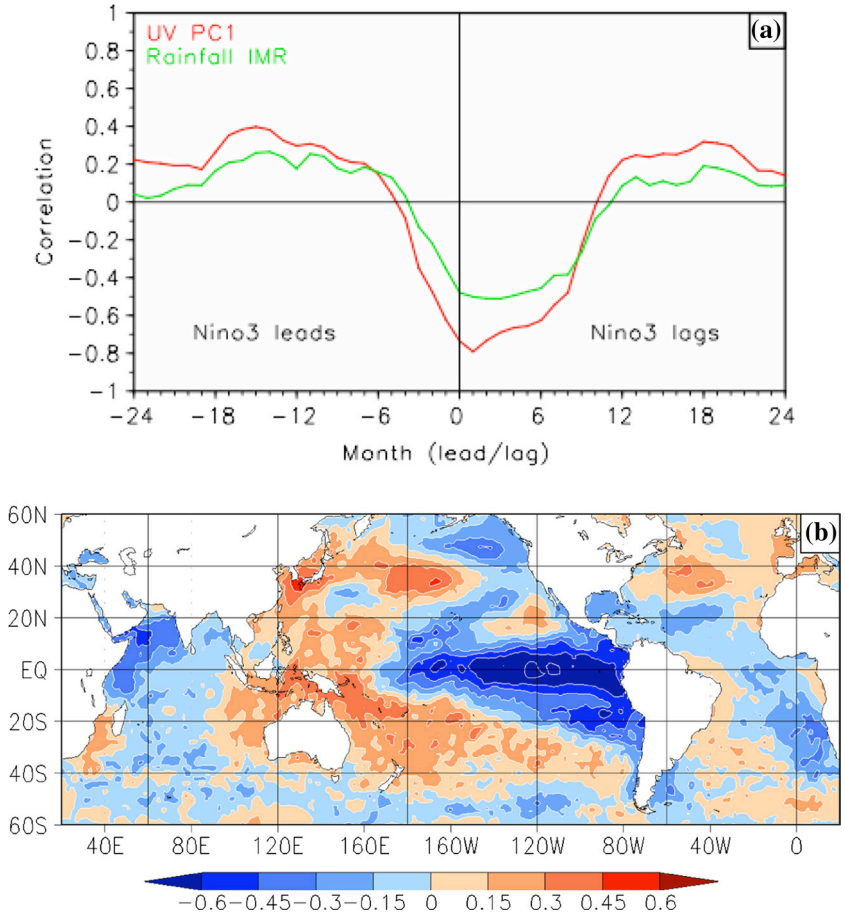

Figure 6
(a) Lag correlation of monthly anomalies of NINO3 index with PC-1 (red) and JJAS seasonal anomaly of IMR index (green) for the period 1948–2003. (b) Point correlation of PC-1 with JJAS seasonal anomaly of SST.

The overall shape of the curve, with weak positive correlation of NINO3 leading the monsoon, followed by a significant negative correlation at zero and small positive lags (monsoon leading NINO3), is quite similar to Figure 19b of WEBSTER *et al.* (1998). The red curve in Figure 6a shows the equivalent lag correlation of NINO3 with the PC of EOF-1. The strong negative correlation at zero lag indicates that the leading circulation mode is strongly SST driven, while the more modest (but significant) correlations with NINO3 leading PC-1 by one or two months indicate some predictability based on knowledge of SST alone.

6. Relationship to Intra-Seasonal Variability

The "residual" hypothesis introduced earlier states that the dominant structure of interannual variability (i.e., EOF-1) arises fundamentally from the structures of intra-seasonal variations, and that the effect of varying external forcing (e.g., SST) in a nonlinear system is to change the relative strength of different preferred intra-seasonal modes. A simple paradigm that illustrates this hypothesis was put forward by PALMER (1999), who showed that when a nonlinear system has a probability density function with several maxima (corresponding to preferred patterns), external forcing can change the relative population (or likelihood) of these maxima, leading to a link between year-to-year variations and variability within the season.

A simply way to test this paradigm in the current context is to expand each intra-seasonal state in terms of the seasonal mean EOFs, which form a set of orthogonal basis functions. The leading projection is just that component of the intra-seasonal state that has the same structure as the leading mode of interannual variability in circulation. Repeating this for many intra-seasonal states (see below), we construct the probability distribution function (pdf) of this component during years when the leading mode is strong, when it is weak, and the remaining years. The distinction among these groups of years is made on the basis of PC-1, as before. If this pdf is approximately the same for all three categories of years, that would suggest that at least some of the statistics of intra-seasonal variability are independent of the state of the leading mode of interannual variability.

We construct a series of running 5-day mean rotational horizontal wind fields at 200 and 850 hPa for each JJAS season, and remove the seasonal mean for each year separately. This yields a series of 118 states for each of 56 years (we lose four days at each of the end points). Each of these states is projected onto EOF-1 of the seasonal means, yielding 118 projection coefficients. The procedure is repeated for each year. (We find that 18.5% of the overall variance of the running pentad means is explained by the projection onto EOF-1 of the seasonal mean.) The set of $118 \times 56 = 6608$ projections is separated into three groups, depending on the value of PC-1, as described above. For each group, a separate pdf estimate is constructed using a kernel density approach (SILVERMAN, 1986).

Figure 7 shows the pdf estimates for strong years (solid line), weak years (dashed line) and the "normal" (remaining) years (dotted line). (The pdfs are normalized so that the integral under the curve is 1.0). While there is slight difference between the strong year and normal year pdfs, the weak year pdf is clearly different from the others.[2] In particular the latter shows a larger weight for moderate negative values, as well as added weight at both extreme tails. While the bi-modality suggested by

[2] The difference between the weak year pdf and either the strong or normal year pdf is statistically significant at the 1% level using the Kuiper test (PRESS *et al.*, 1989).

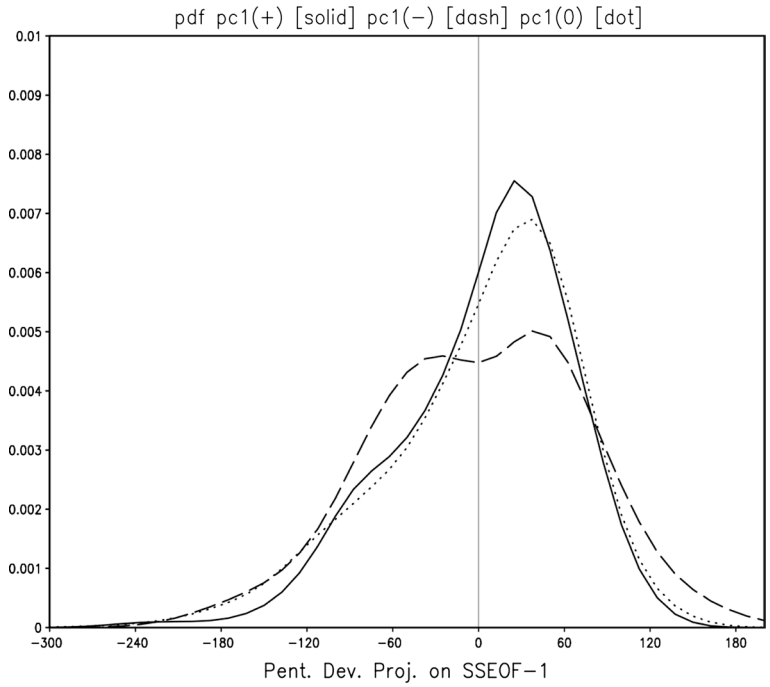

Figure 7

Probability distribution functions (pdfs) of running mean pentad projections of rotational horizontal winds at 850 and 200 hPa on EOF-1. The pdfs are computed separately for (7) strong years (PC-1 > one standard deviation σ) shown in solid line, (12) weak years (PC-1 < $-\sigma$) shown in dashed line, and (37) neutral years, shown in dotted line. The normalization is such that the area under each curve is 1.0. To obtain a dimensional number (in m/sec) from the projections on the x axis, divide by $(N)^{1/2} \sim 41$, with N = 1680 the number of components in the circulation vectors.

Figure 7 may not be statistically significant, there is clear indication that the intra-seasonal statistics during weak years are really different than in other years.

The results suggest that during weak monsoon years the distribution of the component of intra-seasonal variability congruent with EOF-1 of the inter-annual variability is much wider than in other years. This gives partial support to Palmer's paradigm if we assume that the occurrence of a ''weak'' monsoon year is caused by changes in the external forcing (SST).

A more extensive analysis involving an examination of intra-seasonal variations in multiple dimensions is beyond the scope of this paper.

7. Summary and Conclusions

By considering the JJAS seasonal means of the rotational components of the horizontal winds at two levels (850 hPa and 200 hPa), we have shown that the

leading mode of interannual Indian monsoon circulation variability (EOF-1) is highly correlated with the IMR rainfall (correlation of 0.75). This mode shows a strong anti-cyclonic circulation at upper levels and strong Indian Ocean cross-equatorial flow and on-shore flow over western India at lower levels. The monsoon trough is clearly seen in the lower level flow. Composite differences of lower level divergence and vorticity suggest increased rainfall and storminess over the Bay of Bengal and central India when this mode is strong. EOF-2 shows Indian Ocean cross-equatorial flow over a narrower region of the Indian Ocean, and the on-shore flow over western India is more southerly than for EOF-1. The correlation with IMR rainfall is indistinguishable from 0.0.

The multi-level EOF presented here may be compared with a number of other indices based on the circulation, as discussed in the introduction and tabulated in Table 2. The PC associated with the particular EOF we present has a somewhat higher correlation (over a longer period of time) than other circulation measures. More importantly, the EOF incorporates information on vertical shear of the zonal wind (summarizing the first baroclinic mode structure of the monsoon), the vertical shear of the meridional wind (summarizing the modified Hadley circulation) and the full horizontal structure of the low-level cross-equatorial and on-shore monsoon flow.

Composite difference maps of station IMD rainfall over India show a significant signal over central India. For both phases of the EOF-1, the maps of rainfall anomalies are of predominantly one sign over all of India. The spatial structure of the composites is different from the active/break composites of KS and more similar to their strong/weak monsoon year composites.

The point-wise correlation of PC-1 with global seasonal mean SST shows a strong negative correlation over the eastern equatorial Pacific, surrounded by a horse-shoe like pattern of positive correlation, clearly resembling the ENSO signal. Significant negative correlations are seen in the northwestern Indian Ocean. The lag/lead correlation between the NINO3 SST index and PC-1 is very similar to that between

Table 2

Monsoon Indices. Various monsoon indices and their correlation with IMR for JJAS seasonal means. A. Webster-Yang defined originally in Webster and Yang (1992); statistics above from Wang and Fan (1999). B. Monsoon-Hadley defined originally in Goswami et al. (1999); statistics above from Wang and Fan (1999). *C. Westerly shear defined by Wang and Fan (1999). D. PC-1 from EOF analysis presented in Goswami and Ajaya-Mohan (2001). E. PC-4 from EOF analysis presented in Sperber et al. (2000)*

Index Name	Definition	Corr (IMR)	Period
A Webster – Yang	U850 – U200 (0–20N 40–110E)	0.52	1958–1995
B Monsoon–Hadley	V850 – V200 (10–30N 70–110E)	0.64	1958–1995
C Westerly Shear	U850 – U200 (5–20N 40–80E)	0.68	1958–1995
D PC-1 (GM)	(U,V) 850 (20S–30N 40E–100E)	0.62	1958–1997
E PC-4 (S)	(U,V) 850 (20S–40N 60–120E)	0.60	1958–1997
F (this paper)	(Ur,Vr) 850, 200 (12S–42N 50–100E)	0.75	1948–2003

the NINO3 SST index and IMR, but is stronger. Both show modest (but significant) negative correlation when NINO3 leads PC-1 (or IMR) by one-two months, and stronger negative correlations when PC-1 (or IMR) leads NINO3.

The statistics of that component of intra-seasonal variability with the same spatial structure as EOF-1 has been estimated by projecting running five-day means of horizontal rotational winds at 850 and 200 hPa onto EOF-1 (after removing the seasonal mean for each year). The strong and normal pdfs estimated from these coefficients are nearly indistinguishable, but the weak year pdf has more weight for moderate negative values and in both extreme tails.

That the correlations of PC-1 with SST (in particular with NINO3) are at least as strong (if not stronger) than the correlations of SST with IMR itself (compare Fig. 6 with Figure 19b of WEBSTER *et al.*, 1998) suggests a picture in which the slowly varying boundary forcing and large-scale seasonal mean circulation are tightly coupled (as in CHARNEY and SHUKLA, 1981). The actual amount of rainfall occurring locally or over the whole sub-continent, while strongly related to the state of the large-scale seasonal mean circulation, may have some dependence on the statistics of the intra-seasonal variability. The latter point is suggested by Figure 7, which shows the probability distribution of intra-seasonal variability is somewhat altered during low PC-1 (or dry IMR) years.

The rainfall composites (Fig. 5) and the pdfs of Fig. 7 together lend support to the conceptual picture suggested by KS: The interannual variability of the seasonal mean monsoon is a linear combination of large-scale seasonal mean component and a statistical average of intra-seasonal variations.

Acknowledgments

This research was supported by grants from the National Science Foundation (0332910), the National Oceanic and Atmospheric Administration (NA040AR4310034), and the National Aeronautics and Space Administration (NNG04GG46G). The authors thank J. Shukla for encouraging this research.

REFERENCES

CHARNEY, J.G. and SHUKLA, J., *Predictability of monsoons*. In *Monsoon Dynamics* (eds. LIGHTHILL, J. and PEARCE, R.P.) (Cambridge University Press 1981) pp. 99–109.

GOSWAMI, B.N. and AJAYA-MOHAN, R.S. (2001), *Intraseasonal oscillations and interannual variability of the indian summer monsoon*, J. Climate *14*, 1180–1198.

GOSWAMI, B.N., KRISHNAMURTHY V., and ANNAMALI, H. (1999), *A broad-scale circulation index for the interannual variability of the indian summer monsoon*, Quart. J. Royal Meteor. Soc. *125*, 611–633.

KALNAY, E. *et al.* (1996), *The NCEP/NCAR 40-year reanalysis project*, Bull. Am. Meteor. Soc. *77*, 437–471.

KINTER, J.L., FENNESSY, M.J., KRISHNAMURTHY, V., and MARX, L. (2004), *An evaluation of the apparent interdecadal shift in the tropical divergent circulation in the NCEP-NCAR reanalysis*, J. Climate *17*, 349–361.

KRISHNAMURTHY, V. and SHUKLA, J. (2000), *Intraseasonal and interannual variability of rainfall over india*, J. Climate *13*, 4366–4377.

KRISHNAMURTHY, V. and KIRTMAN, B.P. (2003). *Variability of the Indian Ocean: Relation to monsoon and ENSO*, Quart. J. Royal Meteor. Soc. *129*, 1623–1646.

NORTH *et al*. (1982) ■■

PALMER, T.N. (1999), *A nonlinear perspective on climate prediction*. J. Climate *12*, 575–591.

PARTHASARATHY, B., MUNOT, A., and KOTHAWALE, D.R. (1995), *All India monthly and seasonal rainfall series*: 1871–1993, Theor. Appl. Climatol. *49*, 217–224.

PRESS, W.H., TEUKOLSKY, S.A., VETTERLING, W.T., and FLANNERY, B.P. *Numerical Recipes in FORTRAN; The Art of Scientific Computing*, Second Edition (Cambrigde University Press, 1989) pp. 614–622.

RAJEEVAN, M., BHATE, J., KALE, J.D., and LAL, B. (2005), *Development of a high resolution daily gridded rainfall data for the indian region*, Met. Monograph Climatology *22*/2005, National Climate Centre, India Meteorological Department, Pune 411005, India.

RAYNER, N.A., PARKER, D.E., HORTON, E.B., FOLLAND, C.K., ALEXANDER, L.V. ROWELL, D.P., KENT, E.C., and KAPLAN (2003), *A. Global analyses of SST, sea ice and night marine air temperature since the late Nineteenth Century*, in press, J. Geophys. Res. *108*, doi:10.1029/2002JD002670.

SAJI, N.H., GOSWAMI, B.N., VINAYACHANDRAN, P.N., and YAMAGATA. T. (1999), *A dipole mode in the tropical Indian Ocean,* Nature *401*, 360–363.

SPERBER, K.R., SLINGO, J.M., and ANNAMALAI, H. (2000), *Predictability and the relationship between subseasonal and interannual variability during the Asian summer monsoon*, Quart. J. Royal Meteor. Soc. *126*, 2545–2574.

SILVERMAN, B.W., *Density Estimation for Statistics and Data Analysis* (Chapman & Hall, New York, 1986).

STRAUS, D.M. (1983), *On the Role of the Seasonal Cycle*, J. Atmos. Sci. *40*, 303–313.

WANG, B. and FAN, Z. (1999), Choice of south asian summer monsoon indices, Bull. Am. Meteor. Soc. *80*, 629–638.

WEBSTER, P.J. and YANG, S. (1992), *Monsoon and ENSO: selectively interactive systems*. Quart. J. Royal Metor. Soc. *118*, 877–926.

WEBSTER, P.J., MAGANA, V.O., PALMER, T.N., SHUKLA, J., TOMAS, R.A., YANAI, M., and YASUNARI, T. (1998), *Monsoons: Processes, predictability and the prospects for prediction*, J. Geophys. Res. *103* C7, *14*, 451–14,510.

(Received May 20, 2006, accepted November 11, 2006)